

가 가 가

VATER() 가

zoidal) 가 (trape-
(cuneiform) (2) (Fig. 1).

(, 2
) (,)
(1).

(anomalies of the vertebral body)

(butterfly vertebra)
3 6 (somite)
가 12 mm 가
가

(hemivertebra)

가 (2, 3).
가 (3).
가
가 (Fig. 2).
(hypoplasia)

가 (pedicle) (6).
 'C', (neural arch)
 (osseous fusion)
 (end - plates)
 (1).
 가 가
 (4). 가
 (supernumerary) 가
 (scoliosis) 가 (1).
 (cupid bow deformity)
 3, 4
 (5). 5
 (block vertebra)
 (segmentation)
 (Fig. 3).
 (7).
 (facet joint)

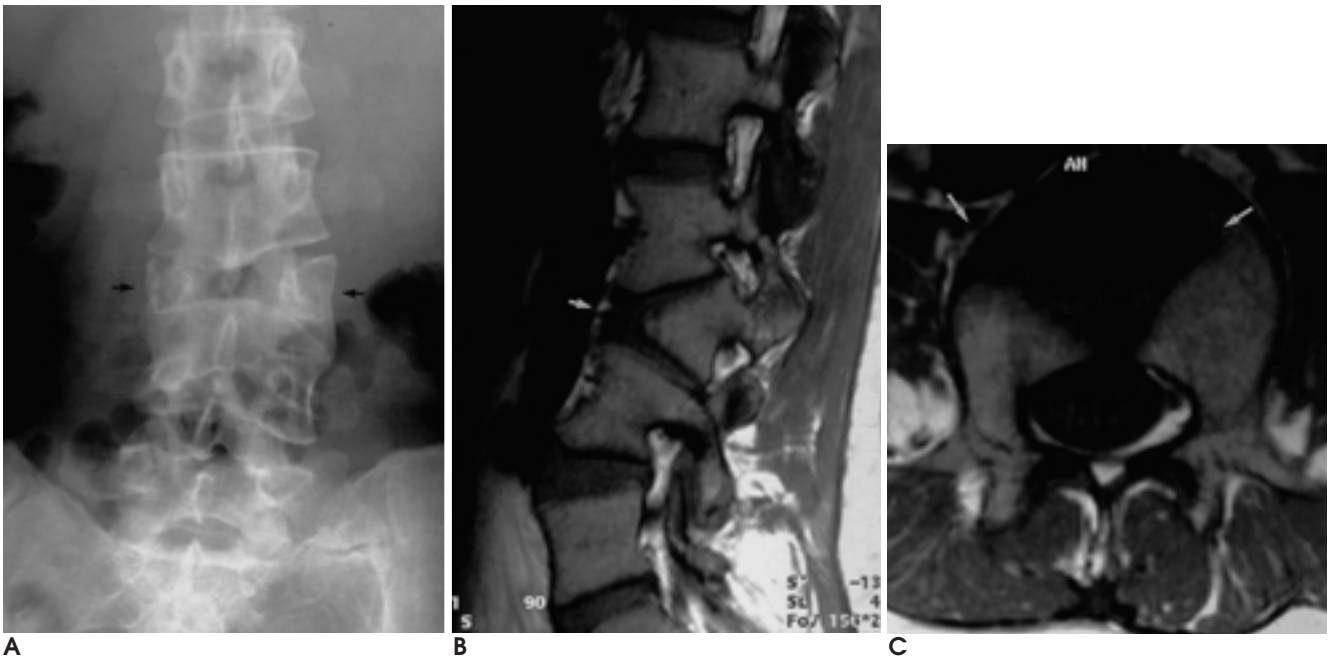


Fig. 1. “ Butterfly vertebra ” in a 38-year-old woman.
A. Anteroposterior radiograph shows sagittal cleft of the third lumbar vertebra (arrows), with an associated compensatory elongation of the adjacent vertebra.
B. Sagittal T1 weighted image demonstrates cuneiform anterior wedging of the third lumbar vertebra (arrow) with the normal posterior border.
C. Axial T1 weighted image shows the cleft (arrows), dividing the body into two lateral halves.

(Fig. 4).

(Schmorl's node)

(megalonuclei polposi)

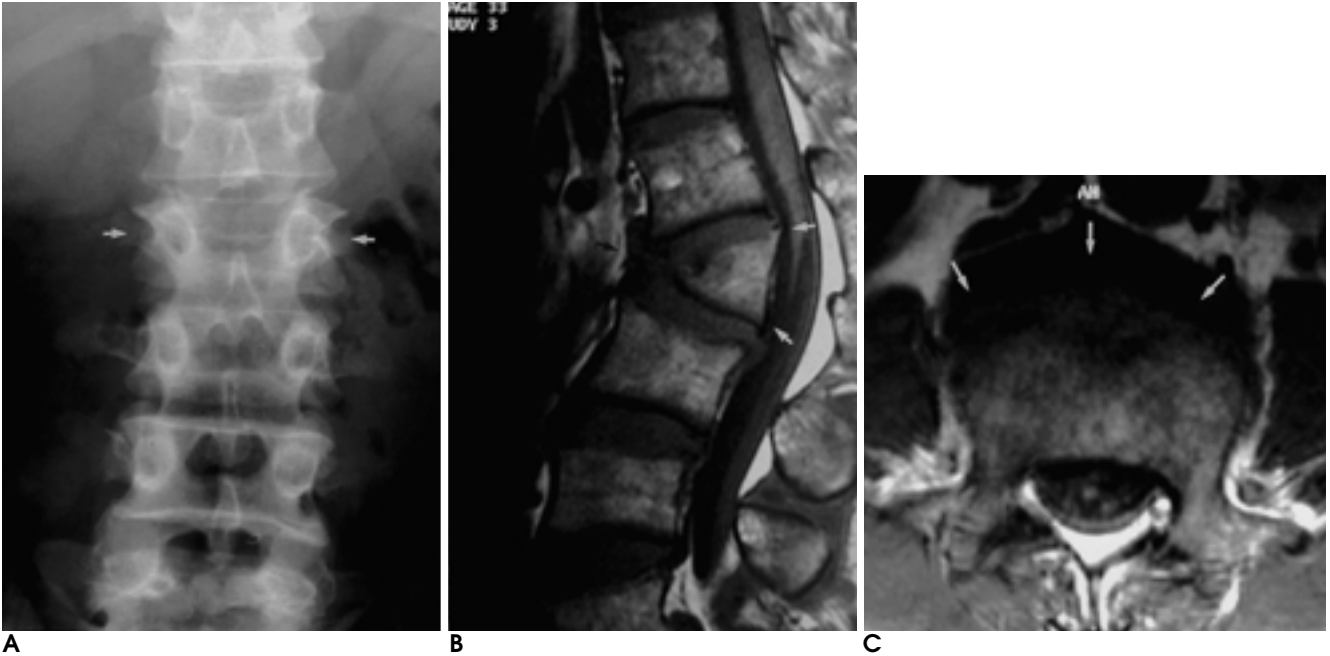


Fig. 2. "Dorsal hemivertebra" of a 43-year-old male.

A. Anteroposterior radiograph shows decreased height of the second lumbar vertebral body (arrows).

B. Sagittal T1 weighted image demonstrates triangular shape of the second lumbar vertebra (arrows); it causes kyphosis with acute anterior angulation of the lumbar spine.

C. Axial T1 weighted image shows posterior hemivertebra with anterior agenesis (arrows), owing to ossification failure.

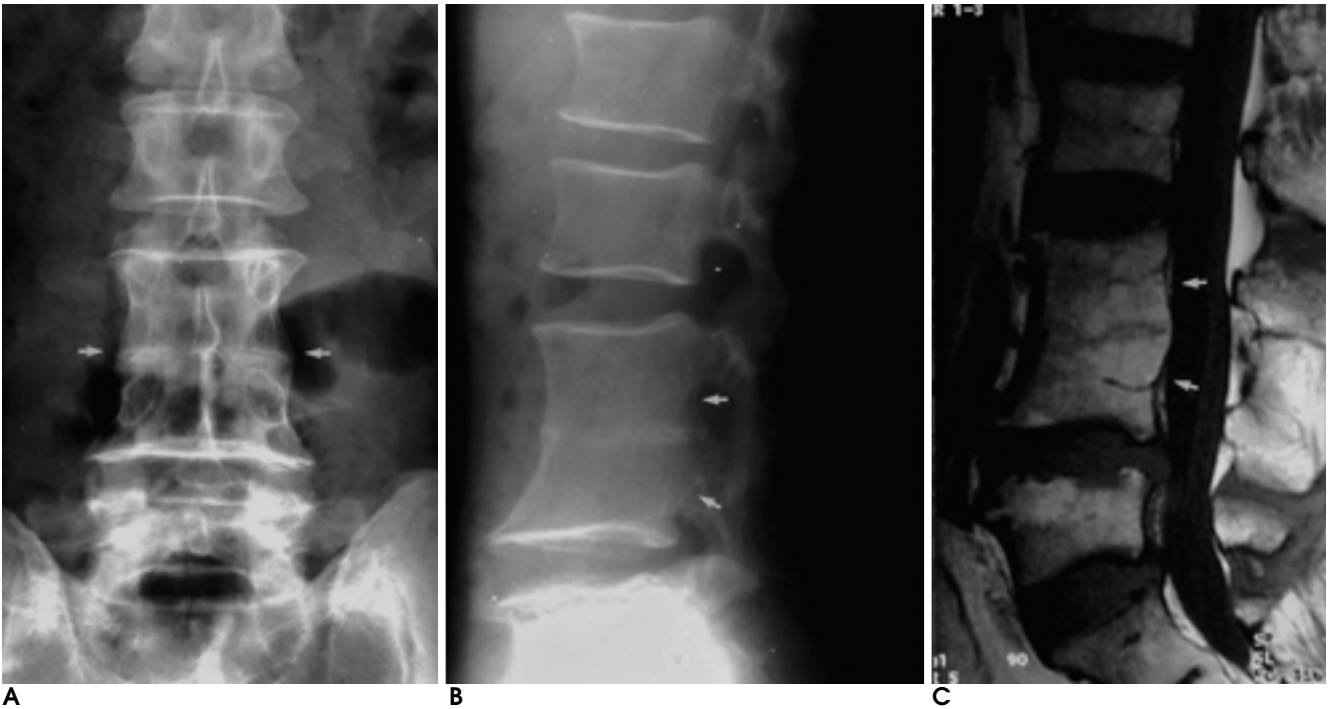


Fig. 3. "Block vertebra" in a 58-year-old man.

Anteroposterior (**A**), lateral (**B**) radiograph and sagittal T1 weighted image (**C**) show fusion of the third and fourth lumbar vertebrae (arrows).

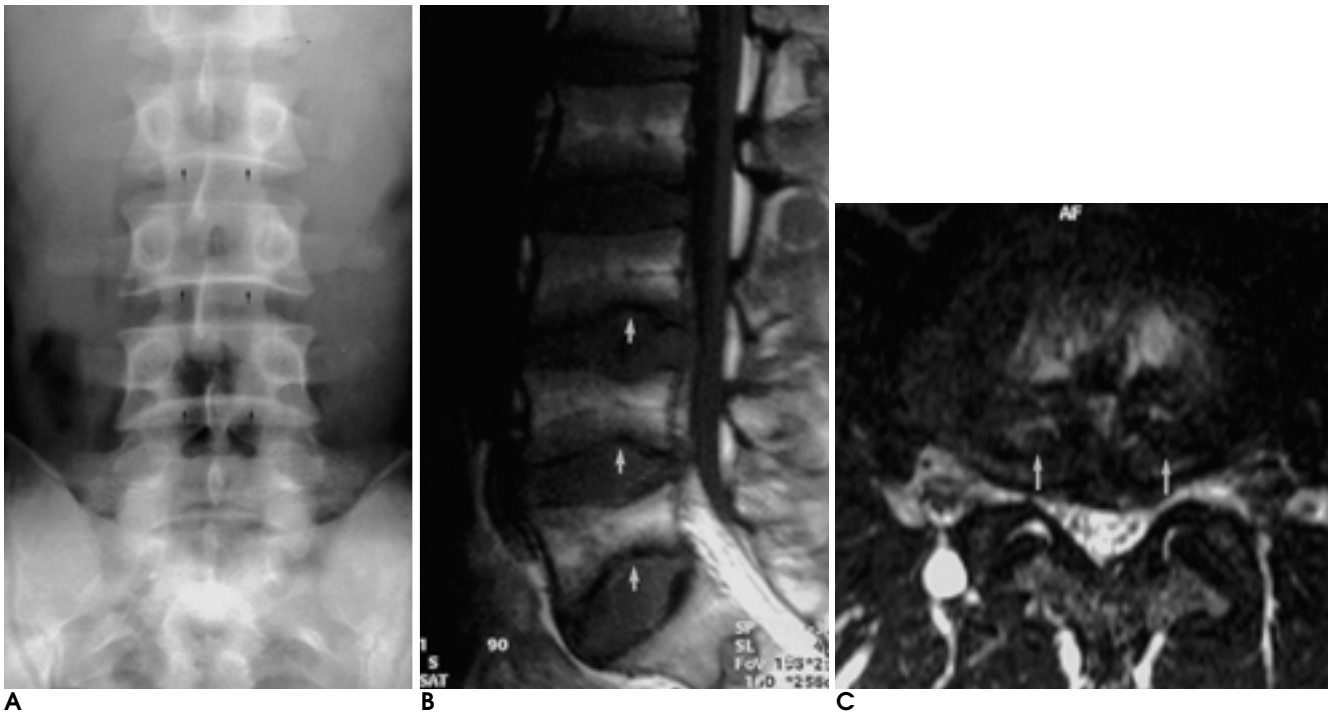


Fig. 4. A 23-year-old man with “Cupid bow deformity.”

A. Anteriorposterior radiograph shows smooth concavities (arrows) on the inferior surfaces of the third to fifth lumbar vertebral bodies.

B. Sagittal T1 weighted image demonstrates concavities (arrows) in the posterior portions of the third to fifth lumbar vertebral bodies.

C. Fat-saturation T2 weighted image shows paired round high-signal intensities (arrows) in the posterior portion of body. These are round areas of the intervertebral disc (‘owl’s eyes’).



Fig. 5. “Hypoplasia of articular process” in a 21-year-old man. Three-dimensional shaded-surface reconstruction of the lumbar spine CT (posterior view) shows hypoplasia of right inferior articular process of the fourth lumbar vertebra. There is an articulation between right superior articular process of the 5th lumbar vertebra and right side lamina of the fourth vertebra (arrows).

(Fig. 4).

(articular process anomaly)

(hypo/hyperplasia of articular process)

가

가

가 3-4

가

2

가

(8).

가

가

가

(9) (Fig. 5).

(10) (Fig. 6).

Roche (11)

가

2

(unfused secondary ossification center)

가

(sesamoid 2

bone), (anomalous accessory bone),

(corticated ossicle)

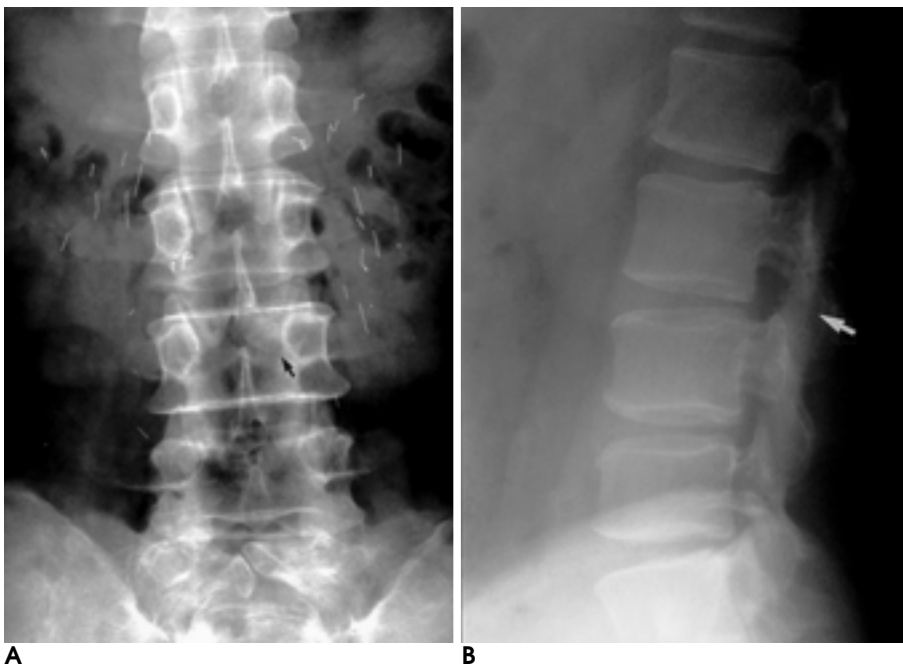
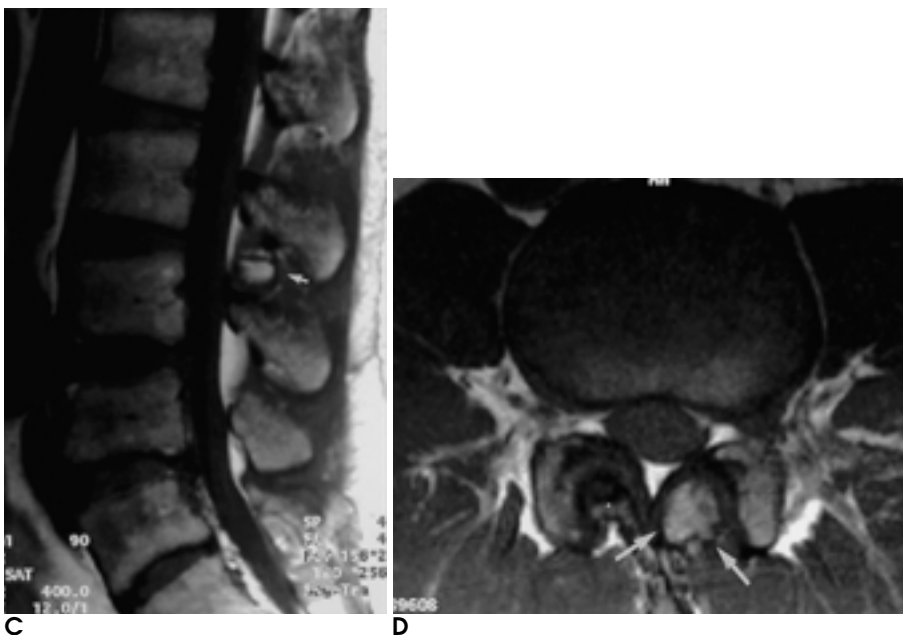


Fig. 6. "Unfused secondary ossification center" in a 34-year-old male.

A. Anteroposterior radiograph shows irregularly margined prominent left inferior articular process of the third lumbar vertebra.

B. It is nearly impossible to define abnormality in lateral view, except subtle obliteration of facet joint between third and fourth lumbar vertebrae (arrow).

C, D. Sagittal T1 weighted image (C) and axial T1 weighted image (D) demonstrate a nonunited apophysis (arrows) of the left inferior articular process of the third lumbar vertebra.



(apophyseal joint)
(10).

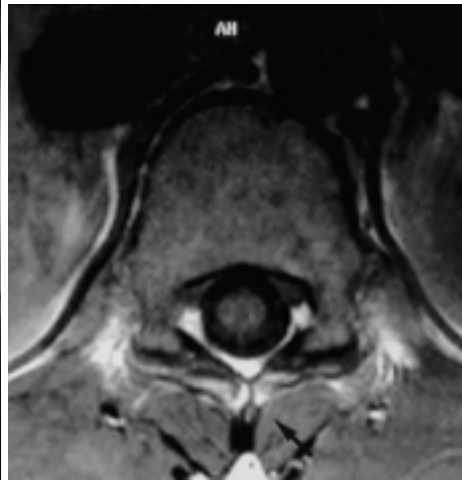
(anomaly of lamina and spinous process)

(spina bifida)

) , 2 가 (



A



B

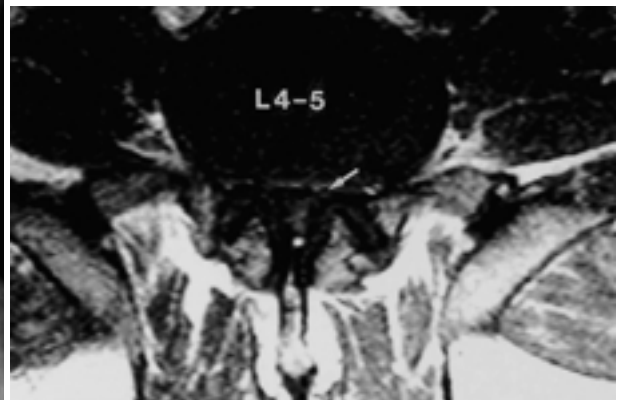
Fig. 7. “ Spina bifida occulta ” in a 24-year-old female. Anteriorposterior radiograph (A) and axial T1 weighted image (B) demonstrate vertical clefts (arrows) in the midline of the posterior neural arch at the eleventh and twelfth thoracic vertebrae.



A



B



C

Fig. 8. “ Achondroplasia of the spine ” of a 42-year-old man. Lateral (A) radiograph shows concave posterior margins of vertebral bodies and wedged vertebrae of the lumbar spine (arrows). Anteriorposterior radiograph (B) and axial T1 weighted image (C) demonstrate decreased interpedicular distance, short pedicle and spinal stenosis (arrow).

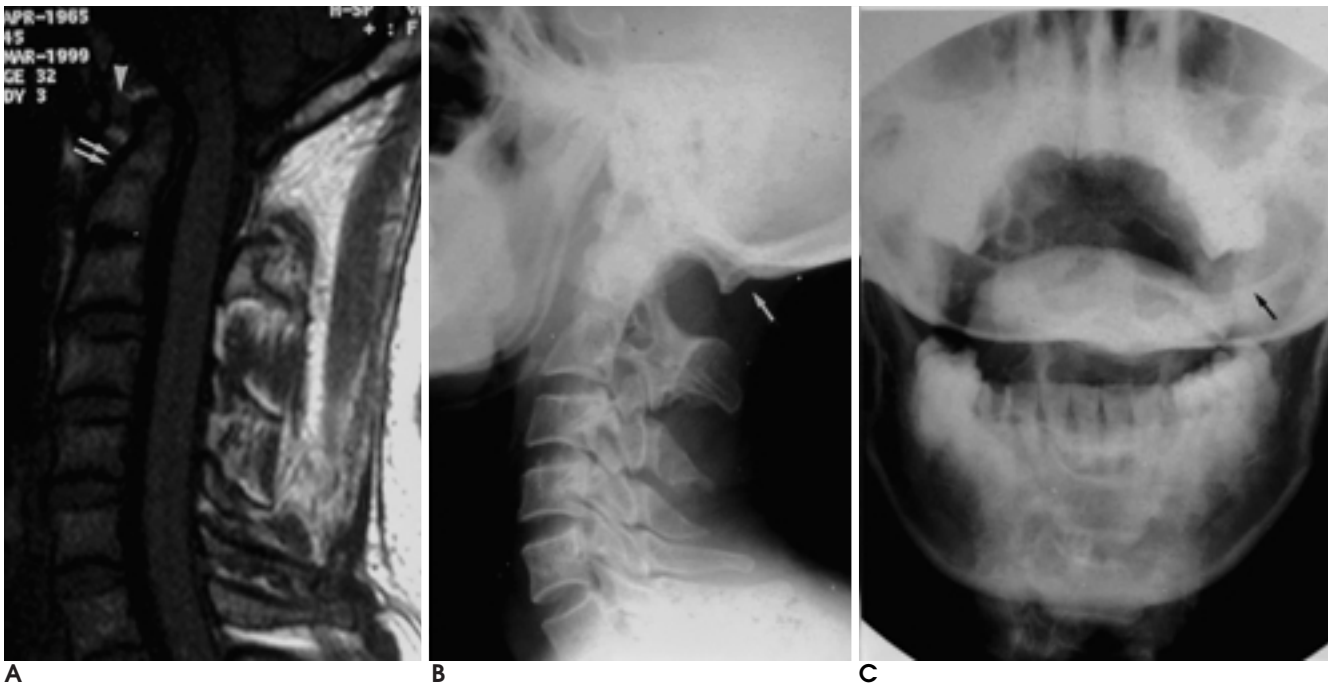


Fig. 9. "Atlanto-occipital assimilation" in a 34-year-old woman. Sagittal T1 weighted image (A), lateral radiograph of the cervical spine (B) and open-mouth radiograph (C) show the fusion of the atlas to the skull base (arrow), incomplete block vertebrae of second and third cervical vertebrae (double arrow) and atlantoaxial subluxation (arrow head).

(1).
 가 (9). 5 1
 11 12 (1)
 (Fig. 7). 5 , 1 1 (sclerotome)
 가 , ()
 (13).
 (fissure line) 2 3 1/2
 (11). 가 (Fig.
 (achondroplasia) 9).
 (endochondral)
 가 가 가

1. Ozonoff MB. Spinal anomalies and curvatures. In Resnick D, Niwayama G. *Diagnosis of bone and joint disorders*. 2nd ed. Philadelphia, W. B. Saunders Company 1988;516-3519
2. Garcia F, Florez MT, Conejero JA. A butterfly vertebra or a wedge fracture? *Int Orthop* 1993;17:7-10
3. Delgado A, Mokri B, Miller GM. Butterfly Vertebra. *J Neuroimag-*

- ing 1996;6:56-58
4. Nasca RJ, Stilling FH 3rd, Stell HH. Progression of congenital scoliosis due to hemivertebrae and hemivertebrae with bars. *J Bone Joint Surg Am* 1975;57:456-466
 5. McMaster MJ, David CV. Hemivertebra as a cause of scoliosis. *J Bone Joint Surg Br* 1986;68:588-595
 6. Guebert GM, Yochum TR, Rowe LJ. Congenital anomalies and normal skeletal variants. In Yochum TR, Rowe LJ. *Essentials of skeletal radiology*. 2nd ed. Baltimore, Williams and Wilkins, 1996; 210-214
 7. Dietz GW, Christensen EE. Normal "Cupid's bow" contour of the lower lumbar vertebrae. *Radiology* 1976;121:577-579
 8. Arcomano JP, Karas S. Congenital absence of lumbosacral articular processes. *Skeletal Radiol* 1982;8:133-134
 9. Klinghoffer L, Murdock MG, Hermel MB. Congenital absence of lumbar articular facets. *Clin Orthop* 1975;106:151-154
 10. Raymond J, Dumas JM. Anomalous ossicle of the articular process: arthrography and facet block. *AJR Am J Roentgenol* 1983;141: 1233-1234
 11. Roche MD, Rowe GG. Anomalous centers of ossification for inferior articular processes of the lumbar vertebrae. *Anat Rec* 1951;109: 253-259
 12. Fitz CR. Diagnostic imaging in children with spinal disorders. *Pediatr Clin North Am* 1985;32(6):1537-1558
 13. Avrahami E, Frishman E, Fridman Z, Azor M. Spina bifida occulta of S1 is not an innocent finding. *Spine* 1994;19(1):12-15

J Korean Radiol Soc 2003;48:345 - 352

Congenital Anomalies of the Spine: Radiologic Findings¹

Jung Kyu Ryu, M.D., Sang Won Kim, M.D., Kyung Nam Ryu, M.D.

¹Department of Diagnostic Radiology, College of Medicine, Kyung Hee University Seoul, Korea

Congenital anomalies of the spine are frequent and variable. Some are restricted to skeletal structures, while others involve combined neural tube defects or are associated with other multi-systemic disorders. Structural spinal anomalies can be classified according to their location: 1) the vertebral body, 2) the articular process, 3) the lamina with spinous process, 4) the pars interarticularis, 5) the facet joint, 6) the pedicle, or 7) other. Because of similarities between these congenital anomalies and (a) secondary changes involving infection or joint disease and (b) deformities resulting from trauma and uncertain tumorous conditions, significant confusion can occur during diagnosis. Moreover, since the anomalies often give rise to both functional impairment and cosmetic problems, appropriate treatment relies crucially on accurate diagnosis. The authors illustrate the pathogenesis and radiologic findings of the relatively common spinal anomalies confined to skeletal structures.

Index words : Spine, anomalies
Spine, radiography
Spine, MR

Address reprint requests to : Kyung Nam Ryu, M.D., Department of Diagnostic Radiology, College of Medicine, Kyung Hee University, 1 Hoegi-dong, Dongdaemun-gu, Seoul 130-702, Korea.
Tel. 82-2-958-8622 Fax. 82-2-968-0787 E-mail: t2star@hanmail.net